A Molecular Orbital Comparison of Molybdenum–Sulfur Dimers with Sulfido Ligands Bridged by CH_2 and FeCp Fragments

D. L. DuBois,*,† F. Kvietok,‡ and M. Rakowski DuBois*,‡

National Renewable Energy Laboratory, 1617 Cole Boulevard, Golden, Colorado 80401, and Department of Chemistry and Biochemistry, University of Colorado, Boulder, Colorado 80309

Received March 25, 1992

An extensive reactivity with hydrogen and unsaturated molecules has been characterized for the μ-sulfide ligands in $(CpMo)_2(\mu\text{-}S)_2S_2CH_2$ (**2**). However, the bridging disulfide ligand in the heteronuclear cluster $[(CpMo)_2(\mu\text{-}S_2)(\mu\text{-}S_2FeCp)]^+$ (**3**) was not reactive toward hydrogen or olefins. Extended Huckel molecular orbital calculations have been carried out for **2** and for the hypothetical Fe–Mo cluster with bridging sulfides rather than a disulfide ligand $[(CpMo)_2(\mu\text{-}S)_2(S_2FeCp)]^+$ (**3′**). The electronic structures of complexes **2** and **3′** are analyzed in terms of the $Cp_2Mo_2S_4$ and methylene and the $FeCp^+$ fragment orbitals, respectively. This approach leads to a qualitative understanding of the reasons for the structural and reactivity differences between **2** and **3**.

Introduction

Cyclopentadienylmolybdenum dimers containing four bridging sulfur atoms have been shown to undergo a wide variety of reactions. At a very early stage in the development of this chemistry, we carried out qualitative molecular orbital calculations for an idealized $Cp_2Mo_2S_4$ dimer, **1**, and two hydrogenated

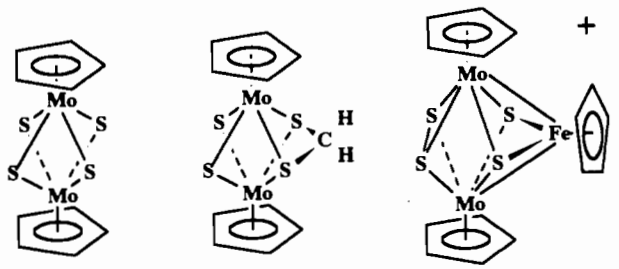

1 **2** **3**

analogues, $[CpMo(\mu\text{-}S)(\mu\text{-}SH)]_2$ and $[CpMo(\mu\text{-}SH)_2]_2$.[1] On the basis of these calculations, the sulfur-based reactivity patterns observed for $[CpMo(SCH_2CH_2S)]_2$ and $[CpMo(\mu\text{-}S)(\mu\text{-}SH)]_2$ could be understood in a qualitative fashion. The preference of the $Cp_2Mo_2S_4$ formulation to form an open structure with two bridging sulfur atoms could also be understood. Other aspects of the $Cp_2Mo_2S_4$ systems have been studied theoretically by a number of groups.[2-7] The subsequent synthesis of $(CpMo)_2(\mu\text{-}S)_2S_2CH_2$[8] (**2**) led to further extensive development of reactivity at the sulfido ligands in this Mo(IV) dimer. The redox chemistry of **2** and its reactions with electrophiles, nucleophiles, and hydrogen have been studied, and catalytic hydrogenation and hydrogenolysis reactions as well as the stoichiometric cleavage of C–S, C–O, and C–N bonds have been characterized.[8-16]

During the course of this work, metallo analogues of **2** were synthesized, e.g., $[(CpMo)_2(\mu\text{-}S_2)(\mu\text{-}S_2FeCp)]^+$ [17] (**3**). Despite the structural similarities between **2** and **3**, the reactivity of the sulfur sites in **3** with unsaturated molecules, with electrophiles and nucleophiles, and with hydrogen was drastically reduced compared to reactivity observed for **2**. In this paper, we examine and compare the electronic structures of **2** and **3** in order to better understand the factors which determine similarities and differences in reactivity.

Results

$(CpMo)_2(\mu\text{-}S)_2S_2CH_2$ (2). We begin our analysis of the electronic structure of **2** by reviewing the frontier orbitals of **1** and the methylene fragment. The frontier orbitals of **1** have been described previously.[1] These orbitals can be divided into three groups on the basis of their symmetry properties in the C_{2v} point group. Group 1 ($1b_2$, $1a_2$, $2b_2$, $3b_2$, $2a_2$) is a set of orbitals that are antisymmetric with respect to the xy mirror plane, as defined in Figure 1, and localized primarily on the molybdenum atoms of dimer **1**. The second group is symmetric with respect to the xy and xz mirror planes and consists of the three a_1 orbitals shown at the right of Figure 1. The third group consists of two b_1 orbitals that are symmetric with respect to the xy mirror plane and antisymmetric with respect to the xz mirror plane. These orbitals are also shown at the right of Figure 1. The frontier orbitals for the bridging methylene group are shown at the left of Figure 1 and consist of a vacant p_y orbital (b_1) and an occupied sp^2 hybrid orbital (a_1) lying on the x axis.

The interaction of $Cp_2Mo_2S_4$ (**1**) with a bridging methylene group is shown in Figure 1. Since the sp^2 and p_y orbitals are symmetric with respect to the horizontal mirror plane of **1**, they have no overlap with the orbitals of group 1. However, the methylene orbitals are of proper symmetry to interact with orbitals of groups 2 and 3. The sp^2 hybrid interacts strongly with the $1a_1$ orbital and weakly with the $2a_1$ and $3a_1$ orbitals of group 2 to produce bonding, antibonding, and two nonbonding combinations.

† National Renewable Energy Laboratory.
‡ University of Colorado.

(1) DuBois, D. L.; Miller, W. K.; Rakowski DuBois, M. *J. Am. Chem. Soc.* **1981**, *103*, 3429.
(2) Bursten, B. E.; Cayton, R. H. *Inorg. Chem.* **1989**, *28*, 2846.
(3) Bruce, A. E.; Tyler, D. R. *Inorg. Chem.* **1984**, *23*, 3433.
(4) Bruce, M. R. M.; Bruce, A. E.; Tyler, D. R. *Polyhedron* **1985**, *4*, 2973.
(5) Newsam, J. M.; Halbert, T. R. *Inorg. Chem.* **1985**, *24*, 491.
(6) Tremel, W.; Hoffmann, R.; Jemmes, E. D. *Inorg. Chem.* **1989**, *28*, 1213.
(7) Stevenson, D. L.; Dahl, L. F. *J. Am. Chem. Soc.* **1967**, *89*, 3721.
(8) McKenna, M.; Wright, L. L.; Miller, D. J.; Tanner, L.; Haltiwanger, R. C.; Rakowski DuBois, M. *J. Am. Chem. Soc.* **1983**, *105*, 5329.
(9) Casewit, C. J.; Haltiwanger, R. C.; Noordik, J.; Rakowski DuBois, M. *Organometallics* **1985**, *4*, 119.
(10) Rakowski DuBois, M. *J. Am. Chem. Soc.* **1983**, *105*, 3710.
(11) Casewit, C. J.; Coons, D. E.; Wright, L. L.; Miller, W. K.; Rakowski DuBois, M. *Organometallics* **1986**, *5*, 951.
(12) Godziela, G.; Tonker, T.; Rakowski DuBois, M. *Organometallics* **1989**, *8*, 2220.
(13) Bernatis, P.; Laurie, J. C. V.; Rakowski DuBois, M. *Organometallics* **1990**, *9*, 1607.
(14) Laurie, J. C. V.; Duncan, L.; Haltiwanger, R. C.; Weberg, R. T.; Rakowski DuBois, M. *J. Am. Chem. Soc.* **1986**, *108*, 6234.
(15) Weberg, R. T.; Haltiwanger, R. C.; Laurie, J. C. V.; Rakowski DuBois, M. *J. Am. Chem. Soc.* **1986**, *108*, 6242.
(16) Lopez, L.; Godziela, G.; Rakowski DuBois, M. *Organometallics* **1991**, *10*, 2660.
(17) Cowans, B. A.; Haltiwanger, R. C.; Rakowski DuBois, M. *Organometallics* **1987**, *6*, 995.

0020-1669/93/1332-0561$04.00/0

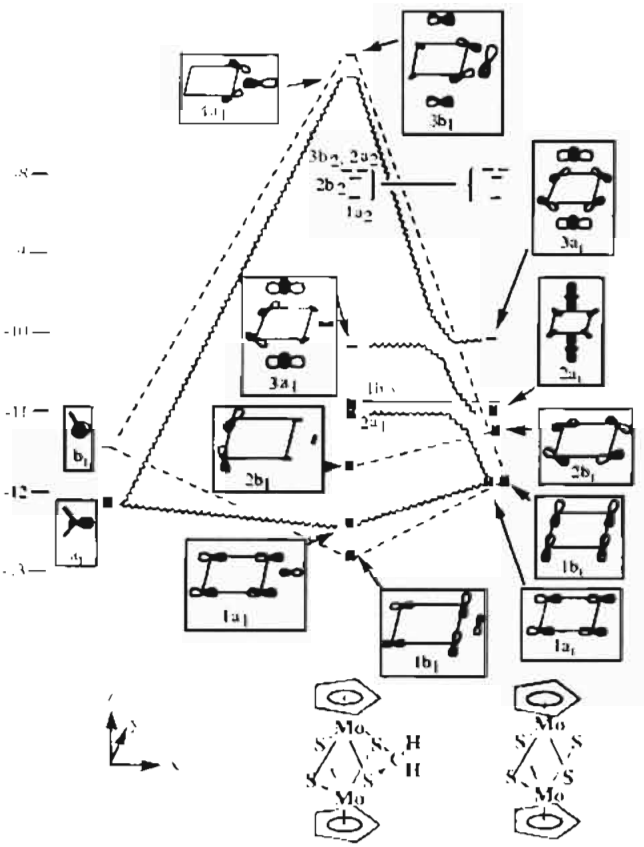

Figure 1. Molecular orbital diagram for $(CpMo)_2(\mu\text{-}S)_2S_2CH_2$ (**2**). See text for discussion. (The x axis has been chosen as the principal axis in order to remain consistent with our previous MO descriptions of related compounds.[1])

These interactions are indicated by the squiggly lines in Figure 1. Three of these orbitals should be occupied. However, the energies of both the antibonding $4a_1$ and nonbonding $3a_1$ orbitals of **2** are considerably higher than the energy of the vacant nonbonding b_2 orbital. Therefore the ground state of the fragments correlates with an excited state of **2** and the interaction of $Cp_2Mo_2S_4$ with the methylene fragment is symmetry forbidden. The formation of complex **2** results in the transfer of two electrons from the a_1 sulfur orbitals in the starting fragment, $Cp_2Mo_2S_4$, to the $1b_2$ metal orbital in $(CpMo)_2(\mu\text{-}S)_2S_2CH_2$ (**2**).

The two b_1 orbitals of group 3 interact with the p_y orbital of the CH_2 fragment to form bonding, nonbonding, and antibonding orbitals (dotted lines in Figure 1). Two of these orbitals are occupied in **2**. In this case, the nonbonding orbital remains within the energy range of the occupied orbitals, and no transfer of electrons between orbitals occurs. The most significant result of the interaction of the methylene group with the $Cp_2Mo_2S_4$ core is the transfer of two electrons from sulfur to the metal-based $1b_2$ orbital. This corresponds qualitatively with our assignment of a +5 oxidation state to the molybdenum atoms of the $Cp_2Mo_2S_4$ fragment and a +4 oxidation state in the methylene bridged dimer, **2**.

Reactivity of 2. Experimental results have demonstrated that the sulfide ligands in **2** reversibly bind olefins;[8] **2** has also been shown to activate H_2 and catalyze HD exchange in hydrogen/deuterium mixtures.[18] The characteristics of these reactions can be considered here because the interaction diagram shown in Figure 1 also applies qualitatively to the reactions of **2** with olefins and hydrogen. This is true because the frontier orbitals of **2** are very similar to those of **1**, and the frontier orbitals of hydrogen and of olefins are similar to those of the methylene fragment. For example, the filled π-bonding orbital of olefins is of a_1 symmetry and corresponds to the sp^2 hybrid of the methylene fragment. The π-antibonding orbital of olefins is a vacant orbital of b_1 symmetry and is an analogue of the p_y orbital of the methylene fragment.

In addition, the frontier orbitals of **2** involve three a_1 and two b_1 orbitals differing only slightly in energy and spatial distribution from those of **1**. The main difference between **2** and **1** is that in the former the $1b_2$ orbital is occupied while in the latter it is not. As a result of the population of this orbital in **2**, the ground state of the reactants will correlate with the ground state of the products, and the reaction of **2** with olefins or H_2 is an allowed process. The interaction involves the vacant low-energy $3a_1$ orbital of **2** acting as an acceptor for a filled σ orbital of H_2 or a π orbital of ethylene and the filled $2b_1$ orbital of **2** back-bonding to the vacant σ-antibonding orbital of H_2 or the π-antibonding orbitals of olefins. The bonding interactions are quite analogous to those used to account for the binding of hydrogen and olefins to a single transition metal via metal d orbitals.

For the reaction of **2** with ethylene, our calculations indicate that the reactants are favored over the products by approximately 5 kcal. This value should not be taken too literally since a full geometry optimization was not performed on either the reactants or the products and because the extended Huckel method is poor at optimizing bond distances. Calculations on the interactions of chlorinated olefins with **2** show favorable binding energies. This would indicate that chlorinated olefins and olefins with other electronegative substituents should form more stable adducts than their hydrogen or alkyl analogues.

An X-ray diffraction study of **2** has not been reported, but in accord with the oxidation state of Mo(IV) assigned above, the complex is assumed to have two bridging sulfide ligands rather than a bridging disulfide ligand. Calculations have shown that formation of a sulfur–sulfur bond in **2** would result in a sharp increase in the energy of the $2b_1$ orbital above that of the lowest unoccupied orbitals. The electrons from this orbital would be transferred to the $3a_1$ orbital. The occupation of the $3a_1$ orbital would result in a repulsive interaction between this filled orbital and the filled π orbital of olefins. The removal of the $2b_1$ orbital from the set of frontier orbitals would result in a loss of the very favorable π-back-bonding interaction with olefins. Therefore a complex with a bridging disulfide ligand is not expected to show the reactivity with olefins and hydrogen that has been observed for **2**.

$[(CpMo)_2(\mu\text{-}S)_2(S_2FeCp)]^+$ (3). The heteronuclear cluster $[(CpMo)_2(\mu\text{-}S_2)(S_2FeCp)]^+$ (**3**) has been synthesized by the reaction of $[MeCpMo(S)(SH)]_2$ with $CpFe(CO)_2I$.[17] Although the gross structure of **3** is similar to that of **2**, an X-ray diffraction study of **3** established that the complex contained a $\mu_2\text{-}\eta^2$-disulfide ligand rather than the two μ-sulfide ligands proposed in **2**. This S–S interaction results in a loss of reactivity as discussed above. The reason for the S–S bond formation in **3** was probed by constructing the molecular orbital diagram of **3'**, in which no S–S bond exists.

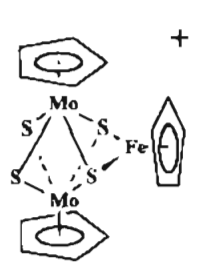

3'

In analogy with the molecular orbital diagram of **2**, the molecular orbitals of **3'** may be constructed from the $Cp_2Mo_2S_4$

(18) Birnbaum, J.; Laurie, J. C. V.; Rakowski DuBois, M. *Organometallics* **1990**, *9*, 156.

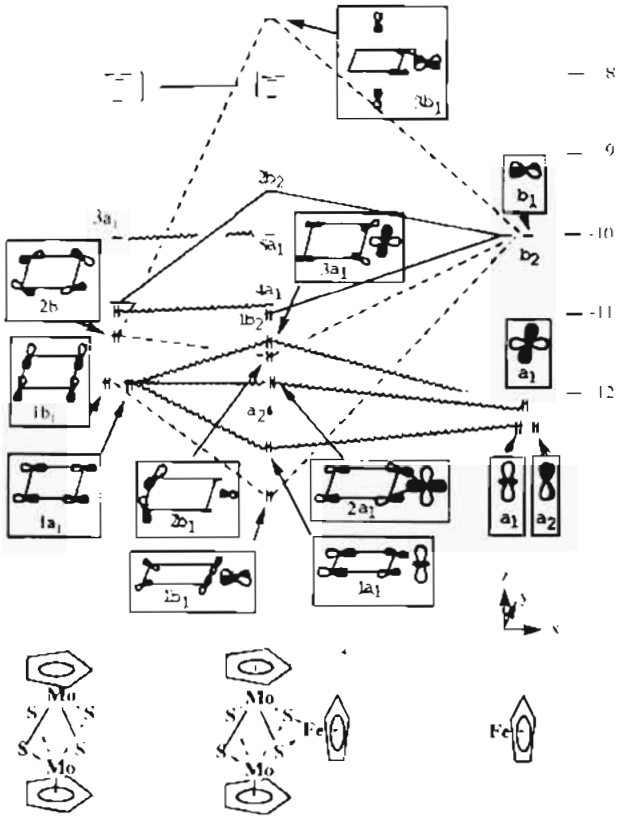

Figure 2. Molecular orbital diagram for $[(CpMo)_2(\mu\text{-}S)_2(S_2FeCp)]^+$ (3′). See text for discussion. (The *x* axis has been chosen as the principal axis.)

core and $FeCp^+$ fragments as shown in Figure 2. The frontier orbitals of $Cp_2Mo_2S_4$ are shown on the left-hand side, and those of $CpFe^+$ are shown on the right. The frontier orbitals of CpM fragments have been discussed in detail elsewhere.[19] They consist of two relatively high-lying metal–Cp antibonding orbitals and three nonbonding orbitals, all of which are localized primarily on the metal. For $FeCp^+$ the three nonbonding orbitals are filled.

From a comparison of Figures 1 and 2 it is clear that an increase in the number of frontier orbitals for the $FeCp^+$ fragment results in a more complex molecular orbital scheme. Many of the new orbitals in Figure 2 are localized primarily on Fe, however. In our discussion, we will focus on the interactions of the set of b_1 orbitals, indicated by dashed lines in Figure 2, and of the set of a_1 orbitals, indicated by squiggly lines, and compare these interactions with their analogues in Figure 1. We will also describe the weak molybdenum–iron bonding interaction in 3′.

The orbitals of group 1 of the $Cp_2Mo_2S_4$ fragment (described above) interact very weakly with the orbitals of the $FeCp^+$ fragment, with the exception of the $1b_2$ orbital. The latter orbital interacts with the d_{xz} orbital of $CpFe^+$ to produce a small stabilization of the molybdenum–molybdenum δ-antibonding orbital and a destabilization of the $CpFe^+$ d_{xz} orbital. The $1b_2$ and $2b_2$ orbitals which result from this interaction are indicated in Figure 2 (solid lines) and are illustrated in the following diagram. The occupation of the $1b_2$ orbital is consistent with

$1b_2$ $\qquad$ $2b_2$

(19) Lauher, J. W.; Elian, M.; Summerville, R. H.; Hoffman, R. *J. Am. Chem. Soc.* **1976**, *98*, 3219.

weak Fe–Mo bonds in the structure. The $2b_2$ orbital is localized primarily on Fe and has no counterpart in the methylene-bridged analogue **2**.

The b_1 (d_{xy}) orbital of the $CpFe^+$ fragment lies along the Fe–S vector and interacts strongly with the b_1 orbitals of **1** in a manner similar to that of the p_y orbital of the methylene fragment. The result again is bonding, nonbonding, and antibonding combinations, as observed for the methylene bridged dimer, **2**. These interactions are shown by the dashed lines of Figure 2.

The three a_1 orbitals of **1** interact with the d_{z^2} and $d_{x^2-y^2}$ orbitals of the $CpFe^+$ fragment and are indicated by squiggly lines in Figure 2. The $2a_1$ and $3a_1$ orbitals of **1** are essentially unperturbed, as is true for the interactions with the methylene fragment shown in Figure 1. The most notable difference between the squiggly lines of Figures 1 and 2 is that the $1a_1$ orbital of **1** interacts only weakly with the $CpFe^+$ $d_{x^2-y^2}$ orbital in a π-antibonding interaction. The resulting $3a_1$ orbital of 3′ is shown in the center of Figure 2. In contrast, the interaction of the $1a_1$ orbital of **1** with the methylene fragment was strong and σ in character, resulting in the high-energy antibonding orbital $4a_1$ of Figure 1. Since the interaction between the $CpFe^+$ $d_{x^2-y^2}$ orbital and the $Cp_2Mo_2S_4$ fragment orbitals is weaker than for the methylene fragment, the antibonding component in 3′ remains lower than the $1b_2$ and $4a_1$ orbitals of 3′. As a result, there are no avoided crossings and no transfer of electrons from predominantly sulfur orbitals to molybdenum orbitals.

The difference between the methylene and $CpFe^+$ fragments can be attributed to two features of the $CpFe^+$ fragment orbitals. First, the d_{z^2} and $d_{x^2-y^2}$ orbitals are of a_1 symmetry in the C_{2v} point group, and some mixing and redistribution occur between these two orbitals upon interaction with the $Cp_2Mo_2S_4$ fragment. Second, the $d_{x^2-y^2}$ orbital is somewhat different than the sp^2 hybrid of the methylene fragment in that it has a nodal plane that lies along the vector joining the Fe and S atoms. This results in a much weaker σ interaction between the $CpFe^+$ and $Cp_2Mo_2S_4$ fragments. Because this weak interaction does not produce the intramolecular redox chemistry observed for **2**, the HOMO and LUMO for complex 3′ are nearly degenerate, as observed previously for **1**.

In the case of **1**, the instability associated with this small HOMO–LUMO gap can be removed by two different distortions. The first involves the formation of a structurally characterized[20] molybdenum dimer containing two bridging and two terminal sulfido ligands. This distortion was discussed in a previous publication.[1] The second distortion which has been demonstrated experimentally[21] and studied theoretically[6] is the formation of a dimer with a sulfur–sulfur bond between two adjacent sulfido ligands. The latter distortion is much more likely for dimer 3′ with the $FeCp^+$ bridge. It is the small HOMO–LUMO gap for 3′ which results in the distortion to form **3**. The formation of a S–S bond in **3** results in a strong antibonding interaction for the $2b_1$ orbital of Figure 2, which leads to a rapid rise in energy of this orbital. As a result, this orbital is removed from the set of frontier orbitals and two electrons are transferred to the $4a_1$ orbital. With the population of the $4a_1$ orbital, the HOMO–LUMO gap has been increased. The removal of the $2b_1$ orbital from the frontier set decreases the ability of the resulting dimer to bind olefins, as discussed above for **2**. The formation of a S–S bond for **3** but not for **2** can therefore be traced to the difference in overlaps observed for the sp^2 hybrid of the methylene fragment and the $d_{x^2-y^2}$ orbital of iron. The weaker interaction of the latter is due to the nodal plane which lies along the sulfur–iron vector.

(20) The structures of $[Cp'MoS(\mu\text{-}S)]_2$ ($Cp' = C_5Me_5$, C_5H_4Me) have been reported: Rakowski DuBois, M.; DuBois, D. L.; VanDerveer, M. C.; Haltiwanger, R. C. *Inorg. Chem.* **1982**, *20*, 3064.

(21) The structure of $(Cp^*Mo)_2(\mu\text{-}S)_2(\mu\text{-}S_2)$ ($Cp = C_5Me_5$) has been reported: Brunner, H.; Meier, W.; Wachter, J.; Guggolz, E.; Zahn, T.; Ziegler, M. L. *Organometallics* **1982**, *1*, 1107.

Discussion

The calculations have derived a set of frontier orbitals which account for the differences in the observed reactivity of the sulfur ligands in **2** and **3**. In **2** a high-lying filled orbital localized primarily on sulfur is of suitable symmetry for back-bonding with the σ-antibonding orbitals of hydrogen or the π-antibonding orbitals of olefins. Complex **2** also contains a low-lying vacant orbital with both metal and sulfur character that has appropriate symmetry for accepting electron density from the σ-bonding orbital of hydrogen or the π-bonding orbital of olefins. The donor–acceptor interactions of the sulfur ligands with olefins are similar to those proposed for transition metal olefin complexes.

Calculations on the interactions of **2** with a series of olefins lead to the conclusion that halogenated olefins and those with other electronegative substituents should form more stable adducts than those of ethylene and its congeners. Experimental tests of this proposed selectivity could lead to a useful separation scheme, e.g., for chlorinated olefins.

Molecular orbital calculations on **3′** showed that the weak nature of the σ interaction of the $CpFe^+$ $d_{x^2-y^2}$ orbital with the $Cp_2Mo_2S_4$ fragment results in a near degeneracy of the HOMO and LUMO in **3′**. Sulfur–sulfur bond formation to form **3** increases the HOMO–LUMO gap and thereby stabilizes **3**. However a consequence of the S–S bond formation is that the sulfur-based orbital, which was dominant in back-bonding interactions with olefins, is highly destabilized and removed from the frontier orbitals of **3**. The calculations provide a consistent framework for understanding why the μ-disulfide ligand in **3** is unreactive toward hydrogen or olefins.

The reduction of **3** by two electrons might be expected to result in the cleavage of the sulfur–sulfur bond. The reduced complex would possess frontier orbitals similar to those of **2** and have a large HOMO–LUMO gap. Thus the anion of **3** might be expected to show reactivity with olefins similar to the reactions observed for **2**, and experimental studies to test this prediction are planned.

Table I. Extended Huckel Parameters

atom	orbital	H_{ij}, eV	ζ_1	ζ_2	C_1[a]	C_2[a]
H	1s	−13.6	1.30			
C	2s	−21.4	1.625			
	2p	−11.4	1.625			
Mo	5s	−8.77	1.96			
	5p	−5.6	1.92			
	4d	−11.06	4.54	1.90	0.5899	0.5899
S	3s	−20.0	1.817			
	3p	−13.3	1.817			
	3d	−8.0	1.50			
Fe	4s	−9.91	1.575			
	4p	−5.07	0.975			
	3d	−12.63	5.35	1.80	0.5366	0.6678

[a] Coefficients used in double-ζ expansion of d orbitals.

Acknowledgment. This work was supported by the Director's Development Fund at NREL and the National Science Foundation at the University of Colorado.

Appendix

Extended Huckel calculations[22] were performed using the weighted H_{ij} formula.[23] The atomic parameters are listed in Table I. The molybdenum parameters were taken from ref 6, and the iron parameters were taken from ref 19. Calculations were performed with and without d orbitals on sulfur. Qualitatively, the calculations were the same. Somewhat better quantitative agreement with the experiment was obtained when d orbitals were used on sulfur. The energy levels shown in Figures 1 and 2 are for calculations performed with d orbitals on sulfur. The bond angles and distances used for the $Cp_2Mo_2S_4$ core were taken from ref 1. The C–S distance used for calculations on complex **2** was 1.82 Å and the Fe–S distance in complex **3** was 2.13 Å.

(22) Hoffman, R. *J. Chem. Phys.* **1963**, *39*, 1397. Hoffman, R.; Lipscomb, W. N. *Ibid.* **1962**, *36*, 3179.
(23) Ammeter, J. H.; Burgi, H. B.; Thibeault, J. C.; Hoffman, R. *J. Am. Chem. Soc.* **1978**, *100*, 3686.